Histol Histopathol (2016) 31: 167-176

http://www.hh.um.es

Histology and Histopathology

From Cell Biology to Tissue Engineering

The role of high cholesterol-high fructose diet on coronary arteriosclerosis

Vicki J. Swier, Lin Tang, Mohamed M. Radwan, William J. Hunter III and Devendra K. Agrawal

Center for Clinical and Translational Science, Creighton University School of Medicine, Omaha, NE, USA

Summary. The effect of fructose in conjunction with high cholesterol diet in the development of atherosclerotic lesions in coronary arteries is not well established. Microswine were fed high cholesterol (HC) or a high cholesterol-high fructose (HCHF) diet containing 18-20% calories from fructose. All swine had high levels of serum cholesterol and non-HDL, thickened intima and accumulation of collagen in the coronaries. Swine fed with HC diet had less stenosis in coronary arteries, lower serum levels of non-HDL, triglycerides, cholesterol, and blood glucose than HCHF group. Coronary lesions in the HC swine were not as progressed as in HCHF and showed low LDL-expressed lipid-laden foam cells. The M1/M2 macrophage phenotype in the HCHF swine differed with the progression of atherosclerosis, with higher density of M1-phenotype in HCHF swine. There was high expression of CCR7 (M1-phenotype) in more advanced lesions in the fibrous cap-like areas, whereas M2-macrophages were abundant in the foam-cell cores. These findings suggest that the addition of a fructose to high cholesterol diet accelerates atherosclerotic lesions in coronary arteries with an increase in M1-macrophages and the propensity to develop features of metabolic syndrome.

Offprint requests to: Devendra K. Agrawal, Senior Associate Dean for Clinical and Translational Science, The Peekie Nash Carpenter Endowed Chair In Medicine, CRISS II Room 510m 2500 California Plaza, Omaha , NE68178, USA. e-mail: dkagr@creighton.edu

DOI: 10.1470/HH-11-652

Key words: Atherosclerosis, Coronary plaques, Fructose diet, Macrophages, Metabolic syndrome

Introduction

In the United States, 71% of the diet is composed of dairy products, cereals, refined sugars, refined vegetable oils and alcohol (Cordain et al., 2005). This "Westernized" diet is usually high in processed foods that contain trans- or saturated fats, sugars and cholesterol. Approximately 31.9 million adults in the USA have total serum cholesterol levels greater than 240 mg/dL and approximately 27.9 million adults have diabetes mellitus, diagnosed and undiagnosed combined (Go et al., 2013). The per capita availability of processed foods containing added fats and oils increased 63% from 1970 to 2005 (52.6 versus 85.5 lbs per person, respectively). The per capita availability of added sugars and sweeteners increased 19% from 1970 to 2005 (119.1 versus 141.6 lbs per person, respectively), attributed mainly to corn sweeteners, including high fructose corn syrup (Wells and Buzby, 2008). High fructose corn syrup is usually found in soft drinks, fruit-flavored noncarbonated beverages, baked goods and other processed foods; but is also a component of canned foods, cereals, flavored dairy products, and fast foods (Duffey and Popkin, 2008).

Fructose intake may also be a risk factor for metabolic syndrome. Rats fed a fructose diet developed metabolic syndrome whereas rats fed diets of glucose and starch did not (Nakagawa et al., 2006), and diets composed of fructose have been found to cause impaired

glucose tolerance and insulin resistance (Faeh et al., 2005). Several clinical features characterize metabolic syndrome. These include abdominal obesity, atherogenic dyslipidemia (characterized by elevated triglycerides and low concentrations of HDL levels), elevated blood pressure, insulin resistance, pro-inflammatory state, and a pro-thrombotic state (Grundy et al., 2004). Clinical outcomes of metabolic syndrome are coronary heart disease/cardiovascular disease.

A contributing factor for cardiovascular disease (CVD) is the development of atherosclerosis, a multiple-stage inflammatory disease that thickens arteries due to the accumulation of apolipoprotein B-containing lipoproteins (apoB-LPs) in various vessels and restricts blood circulation. The endothelial cells of these vessels respond to the apoB-LPs by producing chemoattractants that recruit monocytes. In the pre-lesion stage, monocytes adhere to the endothelium of atherosclerotic vessels, begin to infiltrate the intima of these vessels, and phagocytose lipids to eventually become foam cells (Gerrity, 1981). Monocytes can differentiate into macrophages due to macrophage-colony stimulating factor (M-CSF) and further be differentiated into subsets of macrophages (M1, M2) based on the type of cytokines present. As atherogenesis progresses, more macrophages (acting as foam cells) accumulate within the lesion, devouring lipids, and eventually forming a necrotic core.

During the atherogenesis of the disease, different types of macrophages are activated. Macrophages can be differentiated into M1 and M2 subsets based on the type of cytokines present. The M1-phenotype is characterized by pro-inflammatory IFN-γ or TNF-α- polarized macrophages that produce reactive oxygen species and M2-phenotype is characterized by anti-inflammatory IL-4 or IL-13- polarized macrophages. M1-macrophages are generally recruited first after muscle injury (Collins and Grounds, 2001) that may switch to a M2 phenotype ($CX3CR1^{hi}/Ly6C^{-}$ cells differentiated into $F4/80^{+}$ mΦs) after ingesting cellular debris (Arnold et al., 2007). In some studies, M2-macrophages occur in early stages of inflammation but then the phenotype shifts to M1 polarized macrophages in more advanced stages of inflammation. The adipose tissue macrophages isolated from lean control mice were polarized towards an M2 phenotype ($IL\text{-}10^{+}$ and $Arginase\text{-}1^{+}$), whereas the obese, insulin resistant mice had macrophages polarized towards an M1 state with increased expression of iNOS and decreased expression of Arginase-1 (Lumeng et al., 2007).

Thus, it appears that the excess fat and sugar in the "Westernized diets" may be producing the inflammatory response that initiates cardiovascular disease. However, there are no controlled studies comparing the effect of a high fructose diet in the development of atherosclerosis. In this article, we report the comparative effect of high cholesterol diet with and without fructose, which is similar to most consumed diets in the Western world, on the development of coronary artery lesions. In order to better understand the inflammatory process, we examined the infiltration of M1/M2 macrophages in coronary artery atherosclerotic lesions in a swine model. Swine models have advantages over other animal models because swine are phylogenetically and anatomically similar to humans; swine have a similar omnivorous diet to humans; and swine are similar to humans in vascular response to a high fat diet (Hamamdzic and Wilensky, 2013). Miniature swine are especially useful because of their smaller size, their growth rate, and their traceability (Swindle et al., 1994).

Materials and methods

Porcine model

The Institutional Animal Care and Use Committee of Creighton University approved the research protocol (#0930). Swine were housed and cared for according to NIH and USDA guidelines in the Animal Resource Facility of Creighton University. Micro Yucatan™ miniature swine were purchased from Sinclair Bio-resources (Windham, MA).

Three female Yucatan™ miniature swine were fed a control diet (Harlan Teklad Miniswine diet, Madison WI) and three other female Micro Yucatan™ miniature swine were fed a special high cholesterol diet (Gupta et al., 2012). The high cholesterol diet (HC) consisted of 37.2% corn (8.5% protein), 23.5% soybean meal (44% protein), 20% chocolate mix, 5% alfalfa, 4% cholesterol, 4% peanut oil, 1.5% sodium cholate, and 1% lard; with 52.8% of the kilocalories from carbohydrates and 23.1% of the kilocalories from fat. On month 4, the Micro Yucatan™ miniature swine on control diet were switched to a high cholesterol-high fructose diet-HCHF (Harlan Laboratories). The HCHF diet was designed to replicate the high fat diet of the western world. The main ingredients in the HCHF diet were fructose (230g/Kg), casein (195g/Kg), sucrose (127.5g/Kg), cholesterol (40g/Kg), maltodextrin (90 g/Kg), lard (110 g/Kg), coconut oil (110 g/Kg), sodium cholate (15 g/Kg), cellulose (26 g/Kg), hydrogenated vegetable shortening (55 g/Kg), and soybean oil (10 g/Kg); with 18-20% of the kilocalories from fructose and 45% of the kilocalories from fat. The diets were formulated to be isocaloric with each swine receiving approximately 2700-4500 Kcal/day.

Originally, the HCHF swine were to be fed the HCHF diet for at least 26 weeks (6 months), to increase the probability of developing metabolic syndrome, and the HC swine for 26 weeks as comparison. One of the HCHF swine was euthanized after 22 weeks of the diet because of health factors affecting its quality of life. The Institutional Animal Care and Use Committee of Creighton University recommended euthanasia. The other five swine were fed their respective diets for at least 26 weeks.

Venous blood was collected from each swine for complete metabolic and lipid profile. Blood was

collected before the swine were fed the diet, each month of the diet, and right before euthanasia.

Histology

The whole heart was removed and coronary arteries were excised. The right coronary was excised from the aorta to the ventricular branch and both LAD and LCX were excised. Right and left coronaries were fixed in 10% buffered formalin for 24 hours. Then, the tissues were processed in a Sakura Tissue Tek VIP Tissue Processor and embedded in paraffin. The 4.5 µm sections of tissue block were cut and placed on slides. These slides were stained with hematoxylin and eosin (H&E) and Trichrome and Movat Pentachrome stain. The expression of $CD68^+$ cells (macrophages), $CCR7^+$ M1 macrophages, and $CD206^+$ M2 macrophages was evaluated by immunofluorescence (IF). An antigen-specific for LDL was detected by immunohisto-chemistry.

Histological staining

Tissue sections were routinely stained with hematoxylin and eosin; trichrome stained with a Thermo Scientific* Richard-Allan Scientific* Masson Trichrome Kit (Kalamazoo, MI) per the manufacturers' instructions, and pentachrome stained with the American MasterTech Russell-Movat Pentachrome stain kit (Lodi, CA) per manufacturers' instructions.

Immunohistochemistry

Tissue sections on the slides were deparaffinized in xylene, rehydrated in ethanol, and rinsed in double-distilled water. Antigen retrieval was at 95°C for 20 minutes using DAKO Target Retrieval solution (Carpenteria, CA). Then, slides were rinsed in 1xPBS, endogenous peroxidases were blocked in 3% H_2O_2/PBS for 20 minutes, and rinsed again in 1xPBS. Blocking serum from a VECTASTAIN™ ABC kit containing serum rabbit IgG was incubated on slides for 1 hour at room temp. Slides were drained and the primary antibody from Abcam® (Anti-LDL ab14519) was incubated on the slides for 1 hour at room temp. Slides were rinsed in 1xPBS, and secondary antibody from the VECTASTAIN™ ABC kit was incubated on slides for 2 hours at room temp. Slides were rinsed in 1xPBS, and the VECTASTAIN™ ABC-HRP (horseradish peroxidase) was incubated for 30 minutes on the slides at room temp, slides were then rinsed with 1xPBS and DAB (3,3'-diaminobenzidine) from Vector laboratories was added to the slides for 2 to 10 minutes until the brown color of the DAB started to form. After the DAB had developed sufficiently, slides were washed, stained in hematoxylin, rinsed, dehydrated in ethanol and cleared in xylene. Tissue sections were viewed with a Nikon Eclipse Ci microscope and images were photographed with a Nikon DS-L3 camera. These images were captured using the Nikon DS-L3 software.

Immunofluorescence

Tissue sections on the slides were deparaffinized in xylene, rehydrated in ethanol, and rinsed in double-distilled water. Antigen retrieval was at 95°C for 25 minutes using DAKO Target Retrieval solution (Carpenteria, CA), slides were rinsed in 1xPBS, and tissue sections on the slides were incubated in normal goat serum from Vector Laboratories for 2 hours at room temp. Primary antibody from abcam® (Anti-CD68 ab49777, and a combination of either anti-CCR7 ab32527 or Anti-mannose receptor ab64693) was then added overnight at 4°C. On the following day, slides were rinsed in 1xPBS and the secondary antibody (abcam® goat polyclonal to rabbit IgG FITC ab97199 or Invitrogen Alexa-Fluor® 594 goat anti-mouse IgG) was incubated on the slides for 2 hours at room temp. Slides were then rinsed in 1xPBS and Vector laboratories DAPI mounting medium was added to each slide. Tissue sections were viewed with an Olympus BX-51 epi-fluorescent microscope and images were photographed with an Olympus DP71 camera. These images were captured using Olympus DP Controller software with the exposure set to SFL-Auto. The number of $CCD7^+$ cells and $CD206^+$ cells in the sections of coronary artery plaques was counted, based on the positive immuno-reactivity to the antibody, in a blinded manner by two different observers. The distribution and the number of $CCR7^+$ and $CD206^+$ cells were compared within the plaques of the HCHF swine as well as in the plaques of HC swine. The total number of $CCR7^+$ to $CD206^+$ cells was also compared between the swine of both experimental groups.

Statistical analysis

The blood chemistry data and % stenosis data was analyzed by GraphPad Prism 5.0 (GraphPad Software, Inc). The values are presented as mean ± SEM and analyzed using unpaired t-tests. Statistically significant differences were determined at $p<0.05$. The luminal and internal elastic lamina area was measured by NIH ImageJ software (http://rsb.info.nih.gov/ij/) (Gupta et al., 2012). Briefly, percent area stenosis was calculated as [1-(luminal area/internal elastic lamina area)]*100. At least three hematoxylin and eosin-stained sections from the left and right coronary vessels were measured from each swine.

Results

Blood chemistry and weight

The blood chemistry and weight values for each microswine are displayed in Fig. 1 as line and bar graphs. Each line graph corresponds to monthly measurements taken from each microswine during the

10-month period of the study. To compare the HC diet to the HCHF diet, these values were compared with unpaired t-tests (bar graphs). The fasting blood glucose was increased in the HCHF swine compared to HC swine, with mean values of 102±8.4 and 84±4.4 mg/dL, respectively (Fig. 1A). Though this was not a significant increase at the alpha level of 0.05 (p=0.08), there was a considerable trend toward significance; at least two of the HCHF swine had fasting glucose levels above 130 mg/dL (line graph Fig. 1A). The HCHF swine had a highly significant mean difference in weight compared to HC swine (p<0.0001), with the mean body weight of the HC swine at 23±1.6 Kg and the mean body weight of HCHF swine at 70.3±4.5 Kg (Fig. 1B). The difference in weight was visible in month-6 of the study, after two months of the HCHF diet (line graph Fig. 1B). At the time of euthanasia at month-10, the HCHF swine had reached 91 to 95 Kg in weight.

All the other values in the blood chemistry in HCHF swine were significantly increased compared to the HC swine, including serum triglycerides (p=0.002) (Fig. 1C), serum total cholesterol (p=0.001) (Fig. 1D), serum non-HDL (p=0.002) (Fig. 1E), and serum HDL (p=0.01) (Fig. 1F). Elevated triglycerides were first detected in the HCHF swine in month-7, after three months of the HCHF diet (line graph Fig. 1C). Triglycerides peaked at 61 to 66 mg/dL in month-8 (four months of the HCHF diet).

Comparison of histological analysis

The size and appearance of the coronary lesions

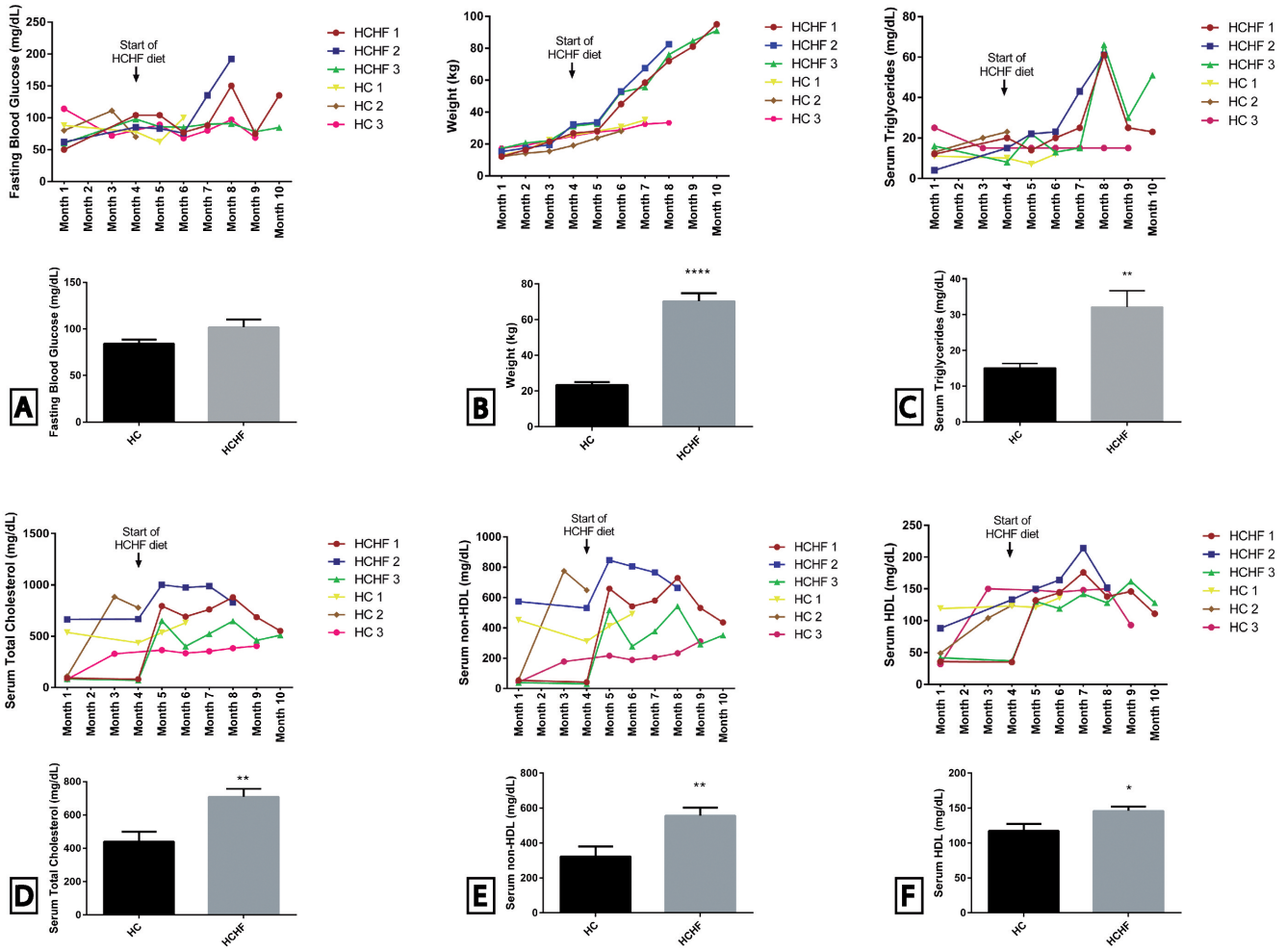

Fig. 1. A comparison of the weight and blood chemistry values between the HC and HCHF swine. Monthly data points of blood chemistry and weight for each microswine are plotted on the line graphs. The values were pooled together and analyzed with unpaired t-tests. The bar graphs are the results of the unpaired t-tests. Results are the mean ± SEM for fasting blood glucose, weight, serum levels of triglycerides, total cholesterol, non-HDL, and HDL. Statistically significant differences between the HCHF and HC swine are shown with asterisk: ****p<0.0001, **p=0.0015, *p=0.01 (n=3 in each experimental group).

differed between the HCHF swine (Fig. 2A,B) and HC swine (Fig. 2C-D). The percent stenosis in the coronary arteries of the HCHF compared to the HC swine was not statistically significant (α=0.05), but had a high trend towards significance at a p value of 0.08. The mean percent stenosis was nearly doubled in the HCHF coronary arteries at 40±7.6%, compared to that in HC coronaries, 22±6.2% (Fig. 2E).

Though there was staining of the LDL antibody in both HCHF (Fig. 2F-G) and HC swine (Fig. 2H-I), the

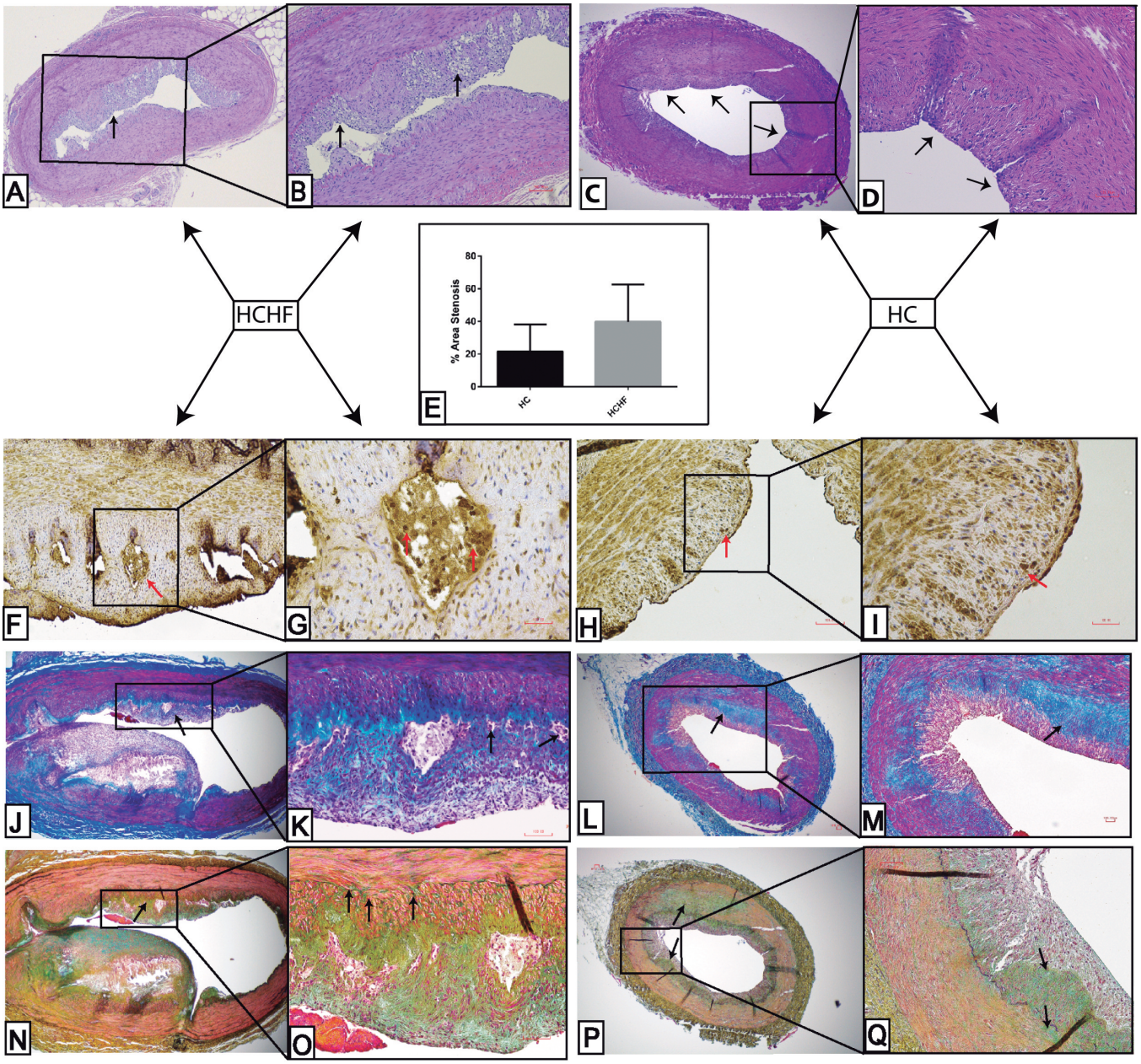

Fig. 2. H&E staining to show histology of coronary arteries of HCHF **(A-B)** and HC **(C-D)** swine. There was intimal thickening in all vessels (note arrows) and greater neointima formation in the HCHF swine (note arrows **A-B**). Mean % area of stenosis in the coronary arteries of HC and HCHF swine was analyzed by unpaired t-tests **(E)**. (n=3 in each experimental group). Immunohistochemistry of LDL in coronaries of HCHF **(F-G)** and HC **(H-I)** swine. Note dark staining of LDL (see arrows) in plaques indicating presence of foam-cells **(G)**. Trichrome staining in the coronary arteries of HCHF (**J-K)** and HC **(L-M)** swine is shown. Note collagen deposition in neointima (arrows **J**) and foam cell layer of HCHF swine (arrows **K)**; and in media of HC swine (arrows **L-M**). Pentachrome staining in the coronary arteries of HCHF (**N-O)** and HC **(P-Q)** swine is shown. The outer proteoglycan layer is visible in the HCHF swine **(N-O)** and fragmentation of elastin (arrows **O**); and proteoglycan deposition within media (arrows **P**) and neointima in HC swine (arrows **Q**). Scale bar: 100 μm.

immunostaining for LDL in the HCHF swine was more concentrated in the outer layer of the lesion and adhered to the remaining foam cells in lipid core areas of the lesion (Fig. 2G). This may indicate that the outer layer is mainly composed of LDL-filled foam cells in the HCHF swine.

In the trichrome staining, all vessels showed deposition of collagen within the muscle layer, as evidenced by blue staining in the tunica media (Fig. 2 J-M). The collagen staining appeared denser at the edge of the tunica media near the initiating point of neointimal formation in the HC swine (Fig. 2L-M). The more advanced lesions of the coronaries in HCHF swine (Fig. 2J-K) resembled those described by Stary (1994) as Type IIa lesions composed of intimal smooth muscles cells containing lipid droplets and an extracellular layer of foam cells. The trichrome stain revealed that the layers of foam cells were interspersed with collagen (Fig. 2K) and the pentachrome staining revealed that the foam cell layer was located at the base of a proteoglycan rich smooth muscle cell layer (Fig. 2O). The intimal smooth muscle cells seemed engorged within the musculoelastic intima (me) and foam cell layer, possibly indicating the presence of lipid droplets (Fig. 2O).

In the Movat's Pentachrome staining, the vessels stained red in the tunica media but there was also light green staining, indicating the accumulation of proteoglycans, in the media of coronary arteries in both HC and HCHF swine (Fig. 2N-Q). The coronaries in the HC swine were in the intimal thickening/pre-lesion stage (Fig. 2P-Q) and did not have the outer proteoglycan layer as seen within the plaque of coronary arteries in HCHF swine (Fig. 2N). In the coronary arteries of both HC and HCHF swine, elastin in all the vessels stained black, but there was a significant loss and fragmentation of the elastin in the coronary arteries of HCHF swine

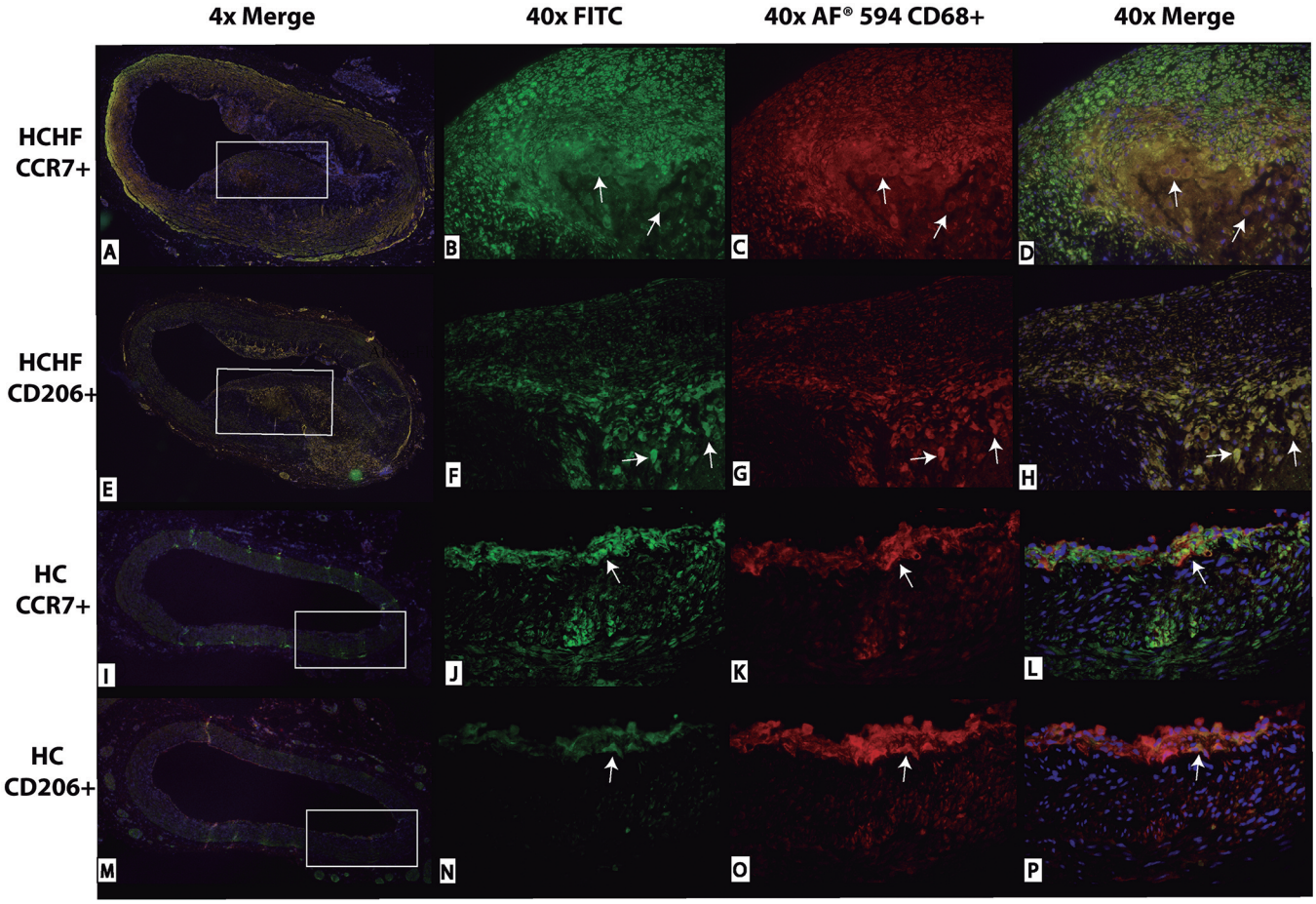

Fig. 3. A-D. Double immunofluorescence staining for CCR7 (marker for M1 macrophages) and CD68 (pan macrophage marker) in HCHF swine. **E-H.** Double immunofluorescence staining of CD206 (marker for M2 macrophages) and CD68 in HCHF swine. **I-L.** Double immunofluorescence staining for CCR7 and CD68 in HC swine. **M-P.** Double immunofluorescence staining for CD206 and CD68 in HC swine. FITC (green) images are either CCR7 **(B and J)** or CD206 **(F and N)**. Cy-3 (red) images are all CD68. Note bright fluorescence of CCR7 (arrows **B**) around the necrotic core of the atheroma and bright fluorescence of CD206 within the necrotic core (arrows **F**) of the atheroma. Comparison of the FITC intensity in **(J)** versus **(N)** reveals that more cells were expressing CCR7 compared to CD206 in HC swine (see arrows). A, E, I, M, x 40; B-D, F-H, J-L, N-P, x 400.

(Fig. 2O).

Immunofluorescence

In the HCHF swine, the immunoreactivity to the CCR7 antibody was present in the tunica media/intima of coronary arteries (Fig. 3A) and to cells in the fibrous cap (Fig. 3B). Interestingly, the cells near the fibrous cap and surrounding the necrotic core stained positive for both CCR7 (Fig. 3B) and CD68 (Fig. 3C), producing a yellowish-orange color indicating co-localization of $CD68^+$ and $CCR7^+$ cells and M1 macrophages (Fig. 3D). Staining of CD206 in HCHF swine coronaries was restricted to the center of the atheroma and a portion of the media (Fig. 3E). However, the cells within the necrotic core in the coronary arteries of HCHF swine stained positive for CD206 (Fig. 3F) and CD68 (Fig. 3G), producing the co-localization of $CD68^+$ and $CD206^+$ cells (Fig. 3H), indicating the presence of M2 macrophages.

In the coronary arteries of the HC swine, the immunostaining to CCR7 was present in the tunica media/intima layer (Fig. 3I), but there was staining of the endothelial layer of the lesion to CCR7 (Fig. 3J) and CD68 (Fig. 3K). Both $CCR7^+$ and $CD68^+$ cells were found attached to the endothelial layer (Fig. 3L). Interestingly, there was immunostaining of CD206 to the same endothelial area (Fig. 3M-N), but fewer cells seem to be $CD206^+$ compared to $CCR7^+$ (Fig. 3J). The co-localization of $CD68^+$ cells (Fig. 3O) with $CD206^+$ cells produces a different spectra signature (Fig. 3P) compared to the co-localization of $CD68^+$ cells to $CCR7^+$ cells (Fig. 3L), indicating the prevalence of $CCR7^+$ M1 macrophages over $CD206^+$ M2 macrophages

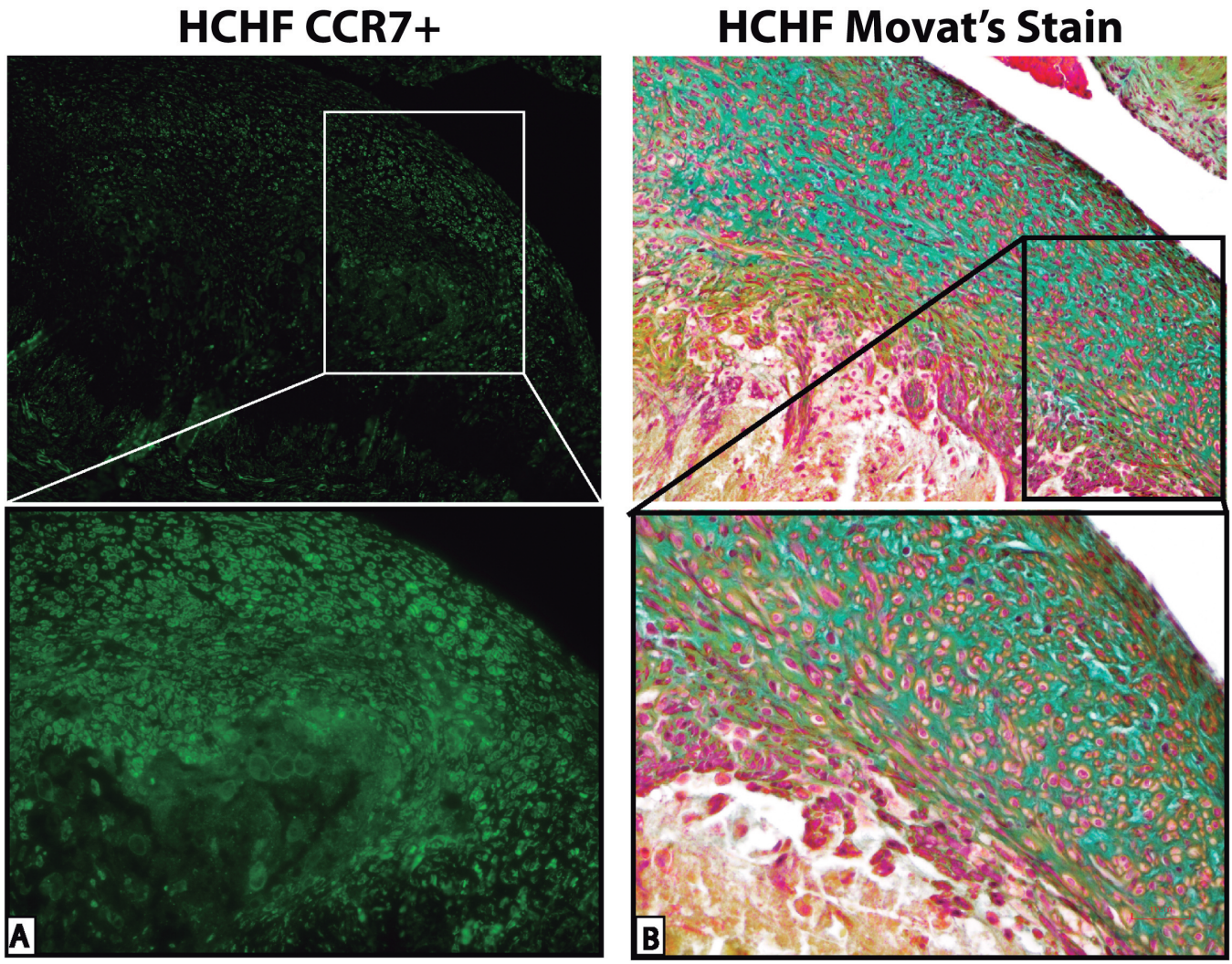

Fig. 4. Comparison of immunofluorescence staining of M1 macrophage marker, CCR7 **(A)** to Movat's pentachrome stain **(B)** in the coronary artery of an HCHF swine. Top row, x 200; Bottom row, x 400.

in the coronary arteries of HC swine.

In the HCHF swine coronary arteries, within the same area of the plaque there was a strong positivity to CCR7 (Fig. 4A) and staining to proteoglycans (as shown by Movat stain) (Fig. 4B).

Discussion

The increase in fat in the HCHF diet may be one of the factors that contribute to higher serum total cholesterol levels with larger and more advanced lesions in the HCHF swine. All swine in this study had intimal thickening and collagen deposition in the coronary arteries and higher than normal serum total cholesterol levels compared to swine fed a normal diet with serum total cholesterol levels from 69 to 119 mg/dL (Gerrity et al., 2001). However, the range of serum total cholesterol levels in the HC swine were lower at 79-778 mg/dL compared to the levels in HCHF swine from 400-1000 mg/dL. All the HCHF swine also had significantly higher weights and mean serum levels for triglycerides, total cholesterol, HDL, and non-HDL than the HC swine; HCHF swine had higher fasting mean blood glucose levels and greater stenosis in the coronary arteries than the HC swine. The lesions that contributed to the stenosis in the HCHF swine were more advanced atheroma with lipid cores, fibrous cap, and signs of necrotic core in the coronary arteries.

In our study, we used a 4% cholesterol diet to promote weight gain and to develop late-stage coronary atheroma in Yucatan miniature swine. In another study by Turk et al. (2005), Yucatan miniature swine diet contained only 2% cholesterol because the objective of their study was to examine early stages of vascular disease. In their study, Turk et al. (2005) reported high levels of both serum cholesterol (greater than 240 mg/dl) and serum LDL (greater than 160 mg/dl), but detected smaller lesions (no significant difference in intima-media thickness compared to control) within the LAD artery and there was no difference in body weights of the swine (44 kg in control versus 45 kg in high fat diet). Goodrich et al. (2003) used 4% cholesterol in Yucatan miniature swine diet and the serum levels of total cholesterol, LDL, and HDL were similar to the Yucatan miniature swine diet with 2% cholesterol. However, the swine fed the 4% cholesterol diet developed intimal lesions greater than 0.5 mm^2 and reached a body weight of 58.7 kg after 26 weeks of the diet. This study supports the use of 4% cholesterol to induce significant atherosclerotic lesions similar to those found in patients with advanced coronary artery disease.

In another study of the cardiovascular artery disease model, the investigators used 1% methionine in conjunction with 0.5% cholesterol to produce atherosclerotic lesions in a rabbit model (Zulli and Hare, 2009) after 4 weeks of the diet. After 12 weeks of the diet, total cholesterol increased and the size of the fibrous cap was 4.8-fold higher than the fibrous caps formed by the cholesterol diet alone. In our studies, we did not use methionine, however, this could be a potential way to induce atherosclerotic lesions in a pig model. However, in our model using a high cholesterol-high fructose diet, there was a significant increase in the levels of serum triglycerides, whereas Zulli and Hare (2009) did not find a significant difference in the blood triglyceride levels between the methionine/cholesterol groups versus the cholesterol diet alone. Nonetheless, further studies are required to compare additional features of metabolic syndrome using methionine in conjunction with 0.5% cholesterol in the diet.

A high fat diet may not be the sole contributor to larger, more advanced atherosclerotic plaques since monosaccharides may also contribute to plaque development. In another study, after 48 weeks of a high fat diet (1.5% cholesterol and 15% lard), diabetic-hyperlipidemic Yorkshire swine (STZ-injected and two doses of 25 g glucose for 2 days) had higher fasting glucose levels (>198 mg/dl) and greater coronary atherosclerosis than nondiabetic-hyperlipidemic swine (Gerrity et al., 2001). The diabetic-hyperlipidemic swine also had a two-fold greater elevation in triglycerides than diabetic-normal diet swine and nondiabetic-hyperlipidemic swine, suggesting a correlation between hypertriglyceridemia and diabetes. Hypertriglyceridemia was also documented in diabetes-induced swine compared to control and high fat diet swine. After 12 weeks of a high fat, high cholesterol diet, alloxan-treated swine had a 2.8-fold increase in triglycerides (mean total triglycerides 0.99±0.30 mmol/L) compared to swine fed a normal diet and swine fed a high fat, high cholesterol diet (Dixon et al., 1999). Both these studies demonstrate that only feeding a high-fat, high cholesterol diet does not result in hypertriglyceridemia in swine.

In this study, we find a hyperglycemia and hypertriglyceridemia profile in HCHF swine with fasting glucose levels that reached 192 mg/dL and triglyceride levels that reached 66 mg/dL (mean serum triglyceride of 32 mg/dL). These findings correlate with the results in non-diabetic-hyperlipidemic swine in published studies (Gerrity et al., 2001) and hyperglycemic male minipigs with fasting plasma glucose levels ranging from 130 to 177 mg/dL fed a high fat, high sucrose diet (Xi et al., 2004). The coronary lesions in the HCHF swine were also similar to those in the nondiabetic-hyperlipidemic swine (Gerrity et al., 2001), and the serum glucose and triglyceride levels were not as high as those reported for the diabetic-high fat, high cholesterol fed swine.

Since high cholesterol- high fructose diet influences the progression of coronary plaques in atherosclerotic swine, there was a change in the phenotype of macrophages that are recruited to these lesions. M1-macrophages ($CCR7^+$ $CD68^+$) were present very early at the pre-lesion stage, as seen in the HC coronaries, attached to the endothelial layer. But, as the lesion progressed and more foam cells were recruited, as seen in the HCHF coronaries, the recruited macrophages expressed both M1 and M2 markers ($CD206^+$ $CD68^+$). At some later point in the atherosclerosis process, when

necrotic cores began to form, M2-phenotype macrophages were found within the necrotic core and M1-phenotype macrophages were scattered around the edges of the necrotic core. The inflammation process may have reached a critical stage and M1-macrophages were needed to recruit inflammatory cytokines, such as TNFα, which induce proliferation and migration of smooth muscle cells to form a thick fibrous cap over the plaque, preventing thrombosis. In the HCHF swine, many of the cells in the upper layer of the plaque were stained positive to CCR7 antibody (M1 marker) and these cells also stained positive for proteoglycans. This outer layer might be serving as a protective fibrous cap composed of CCR7-activated cells and proteoglycans.

Proteoglycans have been associated with lipoprotein deposits in the aorta of non-human primates (Evanko et al., 1998) and the proteoglycan, versican, binds LDL with saturable kinetics (Olin et al., 1999). The distribution of proteoglycans differs based on the stage of the atherosclerotic plaque. In fatty streaks, proteoglycans were found in the subendothelial layer of the foamy macrophage core and in the tunica media, but in more advanced atheroma proteoglycans (especially versican) were found to be distributed in the fibrous cap of the plaque but were missing from the macrophage-filled plaque core (Evanko et al., 1998). We find the same distribution of proteoglycans in the tunica media of atherosclerotic coronary arteries of HC swine and fibrous cap of the atheroma in HCHF swine. The role of proteoglycans in atherosclerotic plaques is still under study, but findings suggest a role of PDGF and/or TGF-β1 in the accumulation of proteoglycans (Evanko et al., 1998), suggesting the role of proteoglycans in smooth muscle cell proliferation (Wight, 2002).

In our study, we document characteristics of atheromas that influence different macrophage recruitment strategies. The change from a M2 anti-inflammatory state to a M1 pro-inflammatory state is based on the progression of the atherosclerotic lesion in swine fed a high cholesterol-high fructose diet. In the HC swine with smaller, less advanced lesions, the macrophages expressed M1 markers ($CCR7^+$ $CD68^+$). Yet, in HCHF swine, when the lesion has become more of an atheroma, macrophages exist in both a pro-inflammatory M1 state and an anti-inflammatory M2 state.

CCR7 immunostaining in advanced lesion of atherosclerotic animals was also observed in plaques from ApoE-/- mice (Damas et al., 2006). The expression of CCR7 positively correlated in a "dose-response" like pattern with the advancement in the lesion. But, in areas of foam-cell-like cells, there was weak expression of CCR7. We find the same pattern in the atheroma of HCHF swine with enhanced expression of CCR7 in the fibrous cap of the atheroma but weak, inconsistent staining of CCR7 in the foam-cell/early necrotic core. All of these factors might be contributing to the destabilization of the plaque.

In conclusion, the combination of high fructose and high cholesterol to a diet contributes to the development of metabolic syndrome as documented by fasting glucose levels greater than 100 mg/dL, elevated triglycerides, and obesity, and increases the progression of advanced plaque formation in the coronary arteries of hypercholesterolemic swine when compared to the coronary arteries of swine fed only a high cholesterol diet. Within the advanced plaques, anti-inflammatory M2 markers accumulate in the core to possibly ingest foam cells, whereas pro-inflammatory M1 markers and proteoglycans within the fibrous cap of the atheroma may recruit cytokines and smooth muscle cells to thicken the cap in order to create a more stable plaque.

In our study, using the high cholesterol-high fructose diet, we found the lesions of non-alcoholic steatosis in the liver, together with insulin insensitivity in one microswine (data not shown). However, this warrants additional careful studies with long-term feeding of high cholesterol-high fructose diet on liver pathology and the pathophysiological features of metabolic syndrome in microswine.

Acknowledgements. The authors thank their colleagues in the laboratory in handling and monitoring swine at various stages of the project. No writing assistance was utilized in the production of this manuscript.

Grants. This work was supported by research grants R01HL116042 and R01HL120659 from the National Institutes of Health, USA to DK Agrawal.

Disclosures. The content of this review is solely the responsibility of the authors and does not necessarily represent the official views of the NIH.

References

Arnold L., Henry A., Poron F., Baba-Amer Y., van Rooijen N., Plonquet A., Gherardi R.K. and Chazaud B. (2007). Inflammatory monocytes recruited after skeletal muscle injury switch into anti-inflammatory macrophages to support myogenesis. J. Exp. Med. 204, 1057-1069.

Collins R.A. and Grounds M.D. (2001). The role of tumor necrosis factor-alpha (TNF-α) in skeletal muscle regeneration: studies in TNF-α (-/-) and TNF-α (-/-)/LT-α (-/-) mice. J. Histochem. Cytochem. 49, 989-1001.

Cordain L., Eaton S.B., Sebastian A., Mann N., Lindeberg S., Watkins B.A., O'Keefe J.H. and Brand-Miller J. (2005). Origins and evolution of the Western diet: health implications for the 21st century. Am. J. Clin. Nutr. 81, 341-354.

Damas J.K., Smith C., Øie E., Fevang B., Halvorsen B., Waehre T., Boullier A., Breland U., Yndestad A., Ovchinnikova O., Robertson A.K., Sandberg W.J., Kjekshus J., Taskén K., Frøland S.S., Gullestad L., Hansson G.K., Quehenberger O. and Aukrust P. (2006). Enhanced expression of the homeostatic chemokines CCL19 and CCL21 in clinical and experimental atherosclerosis. Possible pathogenic role in plaque destabilization. Arterioscler. Thromb. Vasc. Biol. 27, 1-7.

Dixon J.L., Stoops J.D., Parker J.L., Laughlin M.H., Weisman G.A. and Sturek M. (1999). Dyslipidemia and vascular dysfunction in diabetic pigs fed an atherogenic diet. Arterioscler. Thromb. Vasc. Biol. 19, 2981-2992.

Duffey K.J. and Popkin B.M. (2008). High-fructose corn syrup: is this

what's for dinner? Am. J. Clin. Nutr. 88, 1722S-1732S.

Evanko S.P., Raines E.W., Ross R., Gold L.I. and Wight T.N. (1998). Proteoglycan distribution in lesions of atherosclerosis depends on lesion severity, structural characteristics, and the proximity of platelet-derived growth factor and transforming growth factor-β. Am. J. Pathol. 152, 533-546.

Faeh D., Minehira K., Schwarz J.M., Periasamy R., Park S. and Tappy L. (2005). Effect of fructose overfeeding and fish oil administration on hepatic de novo lipogenesis and insulin sensitivity in healthy men. Diabetes 54, 1907-1913.

Gerrity R.G. (1981). The role of the monocyte in atherogenesis: I: transition of blood-borne monocytes into foam cells in fatty lesions. Am. J. Pathol. 103, 181-190.

Gerrity R.G., Natarajan R., Nadler J.L. and Kimsey T. (2001). Diabetes-induced accelerated atherosclerosis in swine. Diabetes 50, 1654-1665.

Go A.S., Mozaffarian D., Roger V.L., Benjamin E.J., Berry J.D., Borden W.B., Bravata D.M., Dai S., Ford E.S., Fox C.S., Franco S., Fullerton H.J., Gillespie C., Hailpern S.M., Heit J.A., Howard V.J., Huffman M.D., Kissela B.M., Kittner S.J., Lackland D.T., Lichtman J.H., Lisabeth L.D., Magid D., Marcus G.M., Marelli A., Matchar D.B., McGuire D.K., Mohler E.R., Moy C.S., Mussolino M.E., Nichol G., Paynter N.P., Schreiner P.J., Sorlie P.D., Stein J., Turan T.N., Virani S.S., Wong N.D., Woo D., Turner M.B. and American Heart Association Statistics Committee and Stroke Statistics Subcommittee. (2013). Heart disease and stroke statistics--2013 update: A report from the American Heart Association. Circulation 127, e6-e245.

Goodrich J.A., Clarkson T.B., Cline J.M., Jenkins A.J. and Del Signore M.J. (2003). Value of the micropig model of menopause in the assessment of benefits and risks of postmenopausal therapies for cardiovascular and reproductive tissues. Fert. Steril. 79, 779-788.

Grundy S.M., Brewer H.B., Cleeman J.I., Smith S.C. and Lenfant C. (2004). Definition of metabolic syndrome. Report of the National Heart, Lung, and Blood Institute/American Heart Association Conference on Scientific Issues Related to Definition. Circulation 109, 433-438.

Gupta G.K., Agrawal T., Del Core M.G., Hunter III W.J. and Agrawal D.K. (2012). Decreased expression of vitamin D receptors in neointimal lesions following coronary artery angioplasty in atherosclerotic swine. PLoS One 7, 1-10.

Hamamdzic D. and Wilensky R.L. (2013). Porcine models of accelerated coronary atherosclerosis: Role of diabetes mellitus and hypercholesterolemia. J. Diabetes Res. 2013, 761415.

Lumeng C.N., Bodzin J.L. and Saltiel A.R. (2007). Obesity induces a phenotype switch in adipose tissue macrophage polarization. J. Clin. Invest. 117, 175-184.

Nakagawa T., Hu H., Zharikov S., Tuttle K.R., Short R.A., Glushakova O., Ouyang X., Feig D.I., Block E.R., Herrera-Acosta J., Patel J.M. and Johnson R.J. (2006). A causal role for uric acid in fructose-induced metabolic syndrome. Am. J. Physiol. Renal Physiol. 290, F625-631.

Olin K.L., Potter-Perigo S., Barrett P.H., Wight T.N. and Chait A. (1999). Lipoprotein lipase enhances the binding of native and oxidized low-density lipoproteins to versican and biglycan synthesized by cultured arterial smooth muscle cells. J. Biol. Chem. 274, 34629-34636.

Stary H.C., Chandler A.B., Glagov S., Guyton J.R., Insull W. Jr, Rosenfeld M.E., Schaffer S.A., Schwartz C.J., Wagner W.D. and Wissler R.W. (1994). A definition of initial, fatty streak, and intermediate lesions of atherosclerosis. A report from the Committee on Vascular Lesions of the Council on Arteriosclerosis, American Heart Association. Circulation 89, 2462-78.

Swindle M.M., Smith A.C., Laber-Laird K. and Dungan L. (1994). Swine in biomedical research: management and models. Farm Anim. Biomed. Res. -Part One 36, 1-5.

Turk J.R., Henderson K.K., Vanvickle G.D., Watkins J. and Laughlin M.H. (2005). Arterial endothelial function in a porcine model of early stage atherosclerotic vascular disease. Int. J. Exp. Path. 86, 335-345.

Wells H.F. and Buzby J.C. (2008). Dietary assessment of major trends in U.S. food consumption, 1970-2005. USDA Economic Information Bull. 33, 1-20.

Wight T.N. (2002). Versican: a versatile extracellular matrix proteoglycan in cell biology. Curr. Opin. Cell. Biol. 14, 617-623.

Xi S., Yin W., Wang Z., Kusunoki M., Lian X., Koike T., Fan J. and Zhang Q. (2004). A minipig model of high-fat/high-sucrose diet-induced diabetes and atherosclerosis. Int. J. Exp. Pathol. 85, 223-231.

Zulli A. and Hare D.L. (2009). High dietary methionine plus cholesterol stimulates early atherosclerosis and late fibrous cap development, which is associated with a decrease in GRP78 positive plaque cells. Int. J. Exp. Pathol. 90, 311-320.

Accepted August 11, 2015